Electrostatic Waves in a Paired Fullerene-Ion Plasma

W. Oohara, D. Date, and R. Hatakeyama
Department of Electronic Engineering, Tohoku University, Sendai 980-8579, Japan
(Received 8 August 2004; published 20 October 2005)

Three kinds of electrostatic modes are experimentally observed to propagate along magnetic-field lines for the first time in the pair-ion plasma consisting of only positive and negative fullerene ions with an equal mass. It is found that the phase lag between the density fluctuations of positive and negative ions varies from 0 to π depending on the frequency for ion acoustic wave and is fixed at π for an ion plasma wave. In addition, a new mode with the phase lag about π appears in an intermediate-frequency band between the frequency ranges of the acoustic and plasma waves.

DOI: 10.1103/PhysRevLett.95.175003 PACS numbers: 52.27.Ep, 52.35.Fp

A typical plasma consists of electrons and positive ions, and an asymmetric diversity of collective plasma phenomena is caused by the large mass difference between electrons and positive ions. On the other hand, a pair plasma consisting of only positive- and negative-charged particles with an equal mass keeps a time-space parity because the mobility of the particles in electromagnetic fields is the same. Positrons have been focused in connection with antimatter property, e.g., CPT invariance, in high-energy physics and astrophysics, and the pair plasma consisting of positrons and electrons has also been investigated theoretically [1–7]. Both the relativistic and nonrelativistic pair plasmas are gradually disclosed to represent a new state of matter with unique thermodynamic properties drastically different from ordinary electron-ion plasmas. Some theoretical works have already been presented, which concern the elementary properties, linear and nonlinear collective modes in nonrelativistic electron-positron plasmas. A comprehensive two-fluid model has been developed for collective-mode analyses, based on which longitudinal/transverse-electrostatic/electromagnetic modes have been studied, and the experimental identification is desired to be performed at present.

The pair plasmas consisting of positrons and electrons have been experimentally produced [8–14]. However, the identification of the collective modes is very difficult in the positron-electron plasmas because the annihilation time is short compared with the plasma period and the plasma density is too low. Therefore our attention is concentrated on the stable generation of a pair-ion plasma consisting of positive and negative ions with an equal mass and the collective-mode identification. According to our previous work on the generation of an alkali-metal–fullerene plasma (K^+, e^-, $C_{60}{}^-$) by introducing fullerenes into a potassium plasma [15–17], fullerenes are adopted as a candidate for the ion source in order to realize the pair-ion plasma, based on the fact that the interaction of electrons with the fullerenes leads to the production of both negative [18,19] and positive [20–22] ions. We have developed a novel method for generating the pair-ion plasma which consists of only positive and negative ions with an equal mass using fullerenes [23], and discuss basic characteristics of the pair-ion plasma in terms of the differences from ordinary electron-ion plasmas. Here the pair-ion plasma source is drastically improved in order to excite effectively the collective modes. In this Letter, we mainly present properties of the electrostatic modes propagating along magnetic-field lines in the pair (-ion) plasma for the first time.

The improved pair-ion source with the ion species of fullerenes is installed in a grounded vacuum chamber of 15.7 cm in diameter and 260 cm in length, as shown schematically in Fig. 1(a). A uniform magnetic field of

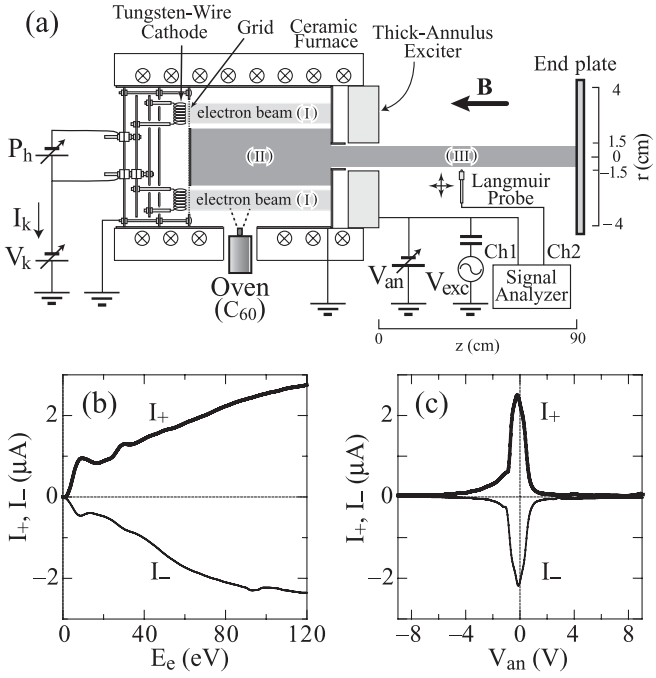

FIG. 1. (a) Schematic drawing of the experimental setup. (b) Generation property of pair-ion plasma depending on electron-beam energy E_e in region (III). (c) Pair-ion density depending on dc-bias voltage V_{an} at $E_e = 100$ eV.

$B = 0.3$ T is applied by solenoid coils and the background gas pressure is 2×10^{-4} Pa. An electron-beam gun is set inside the heated copper cylinder with a thin annulus, which consists of four tungsten wires connected electrically in parallel. This wire cathode heated over 2000 °C by resistive heating is biased at a voltage V_k (< 0 V) with respect to a grounded grid set at less than 0.5 cm in front of the cathode. A stainless-steel disk of 4 cm in diameter is concentrically welded onto the grid anode. Thermionically emitted low-energy electrons (~ 0.2 eV) are accelerated by an electric field between the cathode and the anode, forming a hollow electron beam. The beam flows along magnetic (B) field lines and is terminated at the grounded annulus. The beam energy E_e can be controlled in the range of 0–150 eV by changing V_k. The fullerene vapor is introduced by a fullerene oven from the sidewall of the cylinder, filling the cylinder.

For analytic convenience, the whole space of this plasma is divided into three regions (I), (II), and (III), as shown in Fig. 1(a). The electron-beam region is called region (I) as a fullerene-ion production region. Positive ions C_{60}^+ are produced by the electron-impact ionization and low-energy electrons are simultaneously produced in connection with this process. Negative ions C_{60}^- are produced by the attachment of these low-energy electrons. The electrons and ions are radially separated by a magnetic-filtering effect [24]. Only C_{60}^+ and C_{60}^- are expected to exist in the midmost of the cylinder, region (II), and the electron-free pair-ion plasma generation is attained here. C_{60}^+ and C_{60}^- flow along the B-field lines and pass through the annular hole toward an experimental region, region (III). The thick copper annulus (3 cm in inner diameter, 8 cm in outer diameter, and 3 cm in thickness) is set between region (II) and (III), and independently biased at a dc voltage V_{an} and an ac voltage V_{exc}. The plasma density in region (III) can be controlled by changing V_{an} and V_{exc}. The exit position of the thick annulus is defined as $z = 0$ cm, and the pair-ion plasma is terminated at a floating end plate ($z = 90$ cm). Plasma parameters in region (III) are measured by Langmuir probes, collectors of which are prevented from being contaminated by C_{60}.

The generation property of the pair-ion plasma depending on the electron-beam energy E_e is measured at $r = 0$ cm and $z = 5$ cm in region (III) for $V_{an} = V_{exc} = 0$ V, as shown in Fig. 1(b). I_+ and I_- are the Langmuir-probe saturation currents of C_{60}^+ and C_{60}^-, respectively, which are considered to be in proportion to the ion densities. When E_e increases from 0 eV, the pair-ion plasma begins to be generated, and the plasma density finally attains to maximum 1×10^8 cm^{-3} at $E_e = 100$ eV. The temperatures of C_{60}^+ and C_{60}^-, T_+ and T_-, are about 0.5 eV. The plasma and floating potentials are almost 0 V which is equal to the potential of the grid and the thin annulus. The static potential structures including sheaths are not formed in the pair-ion plasma because the ions have the same mass and temperature. Figure 1(c) gives the plasma density depending on the dc-bias voltage of the thick annulus V_{an} at $r = 0$ cm and $z = 5$ cm for $E_e = 100$ eV and $V_{exc} = 0$ V. Since the density in region (III) drastically decreases for $|V_{an}| \neq 0$ V, the density modulation can be realized without using a grid immersed inside the plasma cross section, which causes the density decrease. Thus, longitudinal-electrostatic modes can be excited in the pair-ion plasma, when the voltage of the annular exciter is temporally alternated ($V_{exc} \neq 0$). Electromagnetic modes relevant to the plasma can be neglected because the density and the temperature are relatively low and the induction current of the ions is very small.

Properties of the wave propagation along the B-field lines are measured at $r = 0$ cm and $z = 10$–12 cm in region (III) for $E_e = 100$ eV by exciting the density fluctuation with the thick annulus, as mentioned above. The measured (dots) and the calculated (solid curves, mentioned below) dispersion relations are shown in Fig. 2, where the density modulation condition is $V_{an} = 0$ V and $V_{exc} = 0.2$ V, and the resultant amplitude of the density fluctuation n_1/n_0 is about 0.1. The wave number (wavelength) is obtained from the phase delay of the positive-ion density fluctuation measured at $z = 10$, 11, and 12 cm. There are three modes in the measured dispersion relation, $\omega/2\pi < 8$ kHz, $8 < \omega/2\pi < 32$ kHz, and $\omega/2\pi > 32$ kHz, where we refer to the modes as the ion acoustic wave (IAW), the intermediate-frequency wave (IFW), and the ion plasma wave (IPW), respectively. IFW has a feature that the group velocity is negative but the phase velocity is positive, i.e., the mode is like a backward wave. The temporal variations of the positive- and negative-ion densities and the potential are measured. The typical temporal

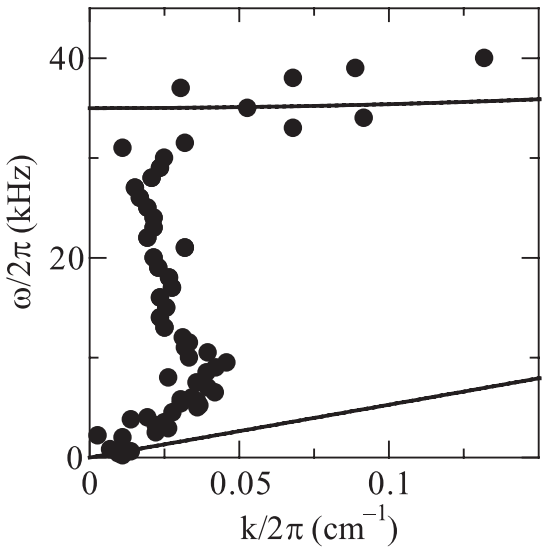

FIG. 2. Dispersion relations for electrostatic waves propagating along B-field lines. Solid lines and dots denote results calculated from two-fluid theory and measured experimentally, respectively.

variations of them are presented for $\omega/2\pi = 0.4$, 20, and 35 kHz in Figs. 3(a)–3(c), respectively. The phase-lag spectrum of the density fluctuations are shown in Fig. 4. $\tilde{I}_+$, $\tilde{I}_-$, and $\tilde{\phi}_f$ indicate the oscillating components of the positive and negative saturation currents (relative to the positive- and negative-ion densities), and the floating potential of the probe (the space potential) measured at $z =$ 10 cm, respectively. The phase lag of the density fluctuation φ for IAW is close to zero and the amplitude of the potential oscillation is extremely small in the very low-frequency range ($\omega/2\pi < 1$ kHz), as seen in Fig. 3(a). The phase lag starts to increase in proportion to $\omega/2\pi$ ($1 < \omega/2\pi < 3$ kHz) and attains a constant value of $\varphi \sim 1.1\pi$ ($3 < \omega/2\pi < 8$ kHz). On the other hand, the phase lags for IPW and IFW are $\varphi = \pi$ and 1.03π, independently of $\omega/2\pi$, respectively. Their potential-oscillation amplitudes are large, as seen in Figs. 3(b) and 3(c). In ordinary electron-ion plasmas, in general, the phase lag is small, i.e., φ is close to zero for IAW. On the other hand, φ is not defined for the electron plasma wave (synonymous with IPW in the pair-ion plasma) because the ion response is very slow compared to electrons and the ion-density fluctuation is ignored. Thus, the waves of $\varphi \simeq \pi$ reflect a special situation. It is accordingly found that IFW has a special property, which is exemplified in a backwardlike mode and a phase inversion of the density fluctuations.

Here we theoretically discuss the experimental results. The two-fluid equations in the absence of an applied B field appropriate to the pair-ion plasma consist of the usual momentum and continuity equations for each species, supplemented with Poisson's equation. Linearizing about a homogeneous unbounded plasma (ion temperatures $T = T_+ = T_-$), and defining the phase lag between the density fluctuations of positive and negative ions by $n_{+1} = n_{-1}\exp(i\varphi)$ for clarity, the coupled linear mode equations are derived:

$$\omega^2 - c_s^2 k^2 - [1 - \exp(-i\varphi)]\omega_p^2 = 0, \tag{1}$$

$$\omega^2 - c_s^2 k^2 - [1 - \exp(i\varphi)]\omega_p^2 = 0, \tag{2}$$

where the acoustic speed $c_s^2 = \gamma T/m$ and the plasma frequency $\omega_p^2 = e^2 n/\varepsilon_0 m$ are introduced. m, n, γ, and ε_0 denote the mass, the density, the ratio of specific heats, and the permittivity of free space, respectively. The dispersion relations associated with Eqs. (1) and (2) are simply given by

$$\omega^2 = c_s^2 k^2 \qquad (\varphi = 0), \tag{3}$$

$$\omega^2 = c_s^2 k^2 + 2\omega_p^2 \qquad (\varphi = \pi). \tag{4}$$

These modes are the ion acoustic wave (3) and the ion plasma wave (4), respectively. In a nonzero applied dc B field but for which a zero magnetic fluctuation, the dispersion relation of modes propagating along B-field lines is quite the same as that in the absence of B field, except for the cyclotron oscillation ω_c and the upper hybrid oscillation $\sqrt{2\omega_p^2 + \omega_c^2}$. The dispersion relation of IFW cannot, though, be derived in this formulation.

The dispersion curves shown in Fig. 2 are calculated using Eqs. (3) and (4) for $\gamma = 3$ (one-dimensional compression), $T = 0.5$ eV (isotropy), and $n_0 = 1 \times 10^7$ cm^{-3}. Here, the pair-plasma frequency is $(\sqrt{2}\omega_p)/2\pi = 35$ kHz, the cyclotron frequency ($B = 0.3$ T) is $\omega_c/2\pi = 6.4$ kHz. In general the ion temperature in the Langmuir-probe measurement is evaluated under the assumption that the velocity distribution functions of the ions are Maxwellian. But the distribution functions in our experiment are likely half-Maxwellian because the ions passing through the exciter hole flow downstream without forming the potential structure which reflects the ions under the collisionless condition. Thus, the distribution function is defined as $f(v) = 2n\sqrt{m/2\pi T}\exp(-mv^2/2T)$ $(v > 0)$, where the thermal velocity is given by $v_{\rm th} = \sqrt{T/m}$ in the case of $-\infty < v < \infty$. In this case the drift velocity is calculated to be $v_d = \sqrt{2T/\pi m}$. The effective thermal velocity is $v'_{\rm th} = \sqrt{(1 - 2/\pi)T/m}$, i.e., the effective

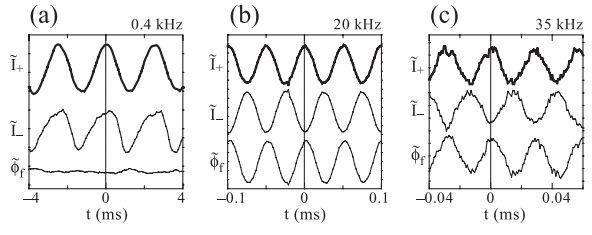

FIG. 3. Typical temporal variations of the densities and potential at $\omega/2\pi =$ (a) 0.4, (b) 20, and (c) 35 kHz. The phase of the negative-ion density is in advance of the positive-ion density.

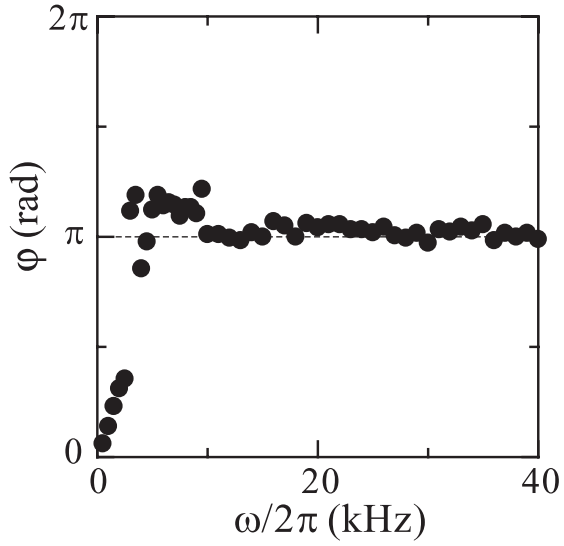

FIG. 4. Phase-lag spectrum of positive- and negative-ion density fluctuations.

temperature is $T' = (1 - 2/\pi)T$. The acoustic speed is $c_s = \sqrt{\gamma(1 - 2/\pi)T/m} = 2.7 \times 10^4$ cm/s. Therefore the phase-velocity comparison between the experiment and theory requires making corrections to allow for this Doppler shift and the effective temperature ($c_s + v_d$). IPW measured fits to the calculated curve, and IAW measured in the relatively low-frequency band ($\omega/2\pi <$ 3 kHz) also fits but deviates from it in the relatively high-frequency band ($3 < \omega/2\pi < 8$ kHz). The phase lag for IAW measured only in the very low-frequency range ($\omega/2\pi < 1$ kHz) is consistent with the theoretical prospects of Eq. (3). The amplitude of the potential oscillation becomes large in proportion to φ because of a charge separation. The phase lag and potential-oscillation amplitude for IPW measured are approximately consistent with the prospects of Eq. (4). The correlation between IAW and IPW does not appear in ordinary electron-ion plasmas because the frequency bands of IAW and IPW are widely different. In the case of the pair-ion plasma, the band of IPW gets close to that of IAW, being accompanied by the appearance of IFW. Thus, the dependency of the IAW phase lag on $\omega/2\pi$ is considered to be caused by the transition from IAW to IFW. Although the existence and property of IFW in the pair-ion plasma is experimentally shown here for the first time, theoretical identification of IFW has not been attained at present. Some theoretical prospects have, however, started to be offered based on our experimental results [25–28], which is significant in light of the ripple effect that our work has provided new knowledge for the community in pair plasmas.

In summary, for the purpose of experimentally investigating electrostatic wave phenomena in a pair-ion plasma, the drastic improvement of the pair-ion plasma source is performed. The active excitation of density modulation by a thick annulus reveals the existence of three kinds of electrostatic modes propagating along B-field lines, an IAW, IPW, and IFW. The properties of IAW and IPW fit to the theoretical one predicted in the two-fluid theory for a unbounded plasma in principle, while IFW experimentally discovered has not been predicted so far. The phase lags between the density fluctuations of positive and negative ions are about π for IFW and IPW, but the phase lag for IAW depends on $\omega/2\pi$.

The authors would like to thank T. Hirata and T. Kaneko for their collaboration. We are indebted to N. Tomioka, M. Kobayashi, and H. Iwata for their support. This work was supported by a Grant-in-Aid for Scientific Research from the Ministry of Education, Culture, Sports, Science, and Technology, Japan.

[1] G. A. Stewart and E. W. Laing, J. Plasma Phys. **47**, 295 (1992).
[2] N. Iwamoto, Phys. Rev. E **47**, 604 (1993).
[3] S. Y. Abdul-Rassak and E. W. Laing, J. Plasma Phys. **50**, 125 (1993).
[4] G. A. Stewart, J. Plasma Phys. **50**, 521 (1993).
[5] J. Zhao, K. I. Nishikawa, J. I. Sakai, and T. Neubert, Phys. Plasmas **1**, 103 (1994).
[6] G. P. Zank and R. G. Greaves, Phys. Rev. E **51**, 6079 (1995).
[7] Daniel H. E. Dubin, Phys. Rev. Lett. **92**, 195002 (2004).
[8] G. Gibson, W. C. Jordan, and E. J. Lauer, Phys. Rev. Lett. **5**, 141 (1960).
[9] C. M. Surko, M. Leventhal, and A. Passner, Phys. Rev. Lett. **62**, 901 (1989).
[10] C. M. Surko and T. J. Murphy, Phys. Fluids B **2**, 1372 (1990).
[11] R. G. Greaves, M. D. Tinkle, and C. M. Surko, Phys. Plasmas **1**, 1439 (1994).
[12] H. Boehmer, M. Adams, and N. Rynn, Phys. Plasmas **2**, 4369 (1995).
[13] E. P. Liang, S. C. Wilks, and M. Tabak, Phys. Rev. Lett. **81**, 4887 (1998).
[14] M. Amoretti *et al.*, Phys. Rev. Lett. **91**, 055001 (2003).
[15] N. Sato, T. Mieno, T. Hirata, Y. Yagi, R. Hatakeyama, and S. Iizuka, Phys. Plasmas **1**, 3480 (1994).
[16] W. Oohara, R. Hatakeyama, and S. Ishiguro, Plasma Phys. Controlled Fusion **44**, 1299 (2002).
[17] W. Oohara, R. Hatakeyama, and S. Ishiguro, Phys. Rev. E **68**, 066407 (2003).
[18] T. Jaffke, E. Illenberger, M. Lezius, S. Matejcik, D. Smith, and T. D. Märk, Chem. Phys. Lett. **226**, 213 (1994).
[19] J. Huang, H. S. Carman, Jr., and R. N. Compton, J. Phys. Chem. **99**, 1719 (1995).
[20] R. Völpel, G. Hofmann, M. Steidl, M. Stenke, M. Schlapp, R. Trassl, and E. Salzborn, Phys. Rev. Lett. **71**, 3439 (1993).
[21] S. Matt, B. Dünser, M. Lezius, H. Deutsch, K. Becker, A. Stamatovic, P. Scheier, and T. D. Märk, J. Chem. Phys. **105**, 1880 (1996).
[22] A. A. Vostrikov, D. Yu. Dubnov, and A. A. Agarkov, High Temp. **39**, 22 (2001).
[23] W. Oohara and R. Hatakeyama, Phys. Rev. Lett. **91**, 205005 (2003).
[24] D. P. Sheehan and N. Rynn, Rev. Sci. Instrum. **59**, 1369 (1988).
[25] A. Hasegawa and P. K. Shukla, Phys. Scr., T **116**, 105 (2005).
[26] P. K. Shukla and L. Stenflo, Phys. Plasmas **12**, 044503 (2005).
[27] F. Verheest and T. Cattaert, Phys. Plasmas **12**, 032304 (2005).
[28] B. Eliasson and P. K. Shukla, Phys. Rev. E **71**, 046402 (2005).